ACS Macro Letters

Letter

pubs.acs.org/macroletters

Hierarchical Self-Assembly of Amphiphilic Homopolymer into Unique Superstructures

Shivshankar R. Mane and Raja Shunmugam*

Polymer Research Centre, Department of Chemical Sciences, Indian Institute of Science Education and Research Kolkata (IISER K), India

Supporting Information

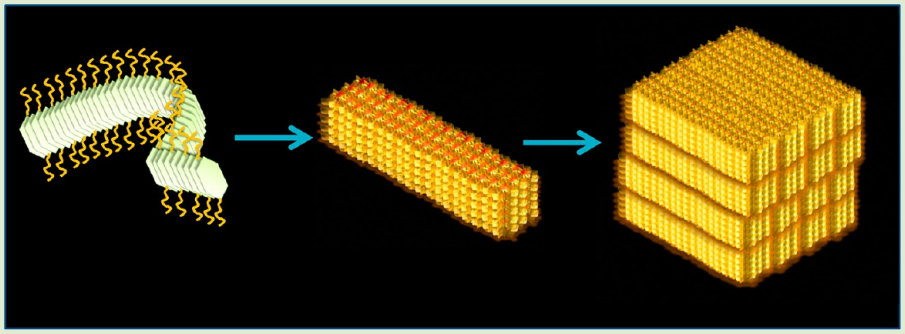

ABSTRACT: Supramolecular forces influence the morphologies of self-assemblies. Herein, self-assembled structures of an amphiphilic, norbornene-derived thiobarbiturate homopolymers (**p-NTB**) are discussed. The newly designed hompolymer shows self-assembled rod-like structures in tetrahydrofuran (THF) solvent. Formation of the rods are governed by hydrogen bonding motifs and amphiphilicity found in the molecular architecture. The solvent polarity controls their organization into cube-like and sphere-like structures at the next length scale. Encapsulation studies of hydrophobic magnetic particles as well as drug molecules into these superstructures demonstrate a novel route to fabricate multifunctional cube-like and sphere-like aggregates.

Self-assembly is a versatile approach for constructing numerous nanosized as well as microsized aggregates.[1] Molecules with hydrophilic and hydrophobic blocks are used to explore assembly behaviors and molecular interactions of amphiphilic molecules.[2] Self-assembly of amphiphilic molecules into novel architectures opens a new avenue for creating materials and devices with unique properties.[3] In particular, nanosized aggregates from block copolymers, especially rod-shaped and patchy aggregates have attracted significant attention.[4] Assembly of rod-shaped aggregates from the multiple blocks can potentially produce a variety of superstructures.[5] This is due to the interaction and competition of the structural asymmetry of rods, and phase segregation of amphiphilic molecules. The self-assembly of such a complex block copolymer systems is well documented for studying phase behavior and the dynamics of micelle formation or biomimetic principles of self-organization observed in biological systems.[6,7]

Recently, worm-like or rod-like micelles are preferred as nanocarriers among the other nano structures due to high loading capacity of hydrophobic objects per micelle as well as long in vivo circulation capabilities.[7] This is done either by melt state or by precipitation.[8] There are well established methods to make core or corona of worm-like as well as cylinderical micelles due to the amphiphilicity in the block copolymers.[2,4] But, this type of hierarchical self-assembly of amphiphilic homopolymers are not explored so far. In this manuscript, the exciting properties of hydrogen bonding systems[9] have been combined with macromolecular amphiphilicity to create a self-assembled aggregates, which hierarchically organizes first into rods in solution and then into cube-like as well as sphere-like structures on a surface as shown by the scanning electron microscopy (SEM), atomic force microscopy (AFM), and transmission electron microscopy (TEM) images in Figures 1−3. The norbornene-derived thiobarbiturate homopolymers (**p-NTB**) have been prepared using ring-opening metathesis polymerization.[10] We have further demonstrated that **p-NTB** homopolymer could spontaneously organize into diverse morphologies in solvent mixtures. To best of our knowledge, this is the first exploration of self-assembly of amphiphilic homopolymers into very unique structures.

The motivation of this study is to investigate the effect of homopolymer amphiphilicity and the solvent polarity on the micelle morphologies, which has, so far, not been explored systematically. We followed the approach of dissolving the **p-NTB** in THF and then adding water or MeOH, which were selective solvents for the polar motif. Therefore, two solvent

Received: October 29, 2013
Accepted: December 18, 2013
Published: December 20, 2013

dx.doi.org/10.1021/mz4005524 | *ACS Macro Lett.* 2014, 3, 44−50

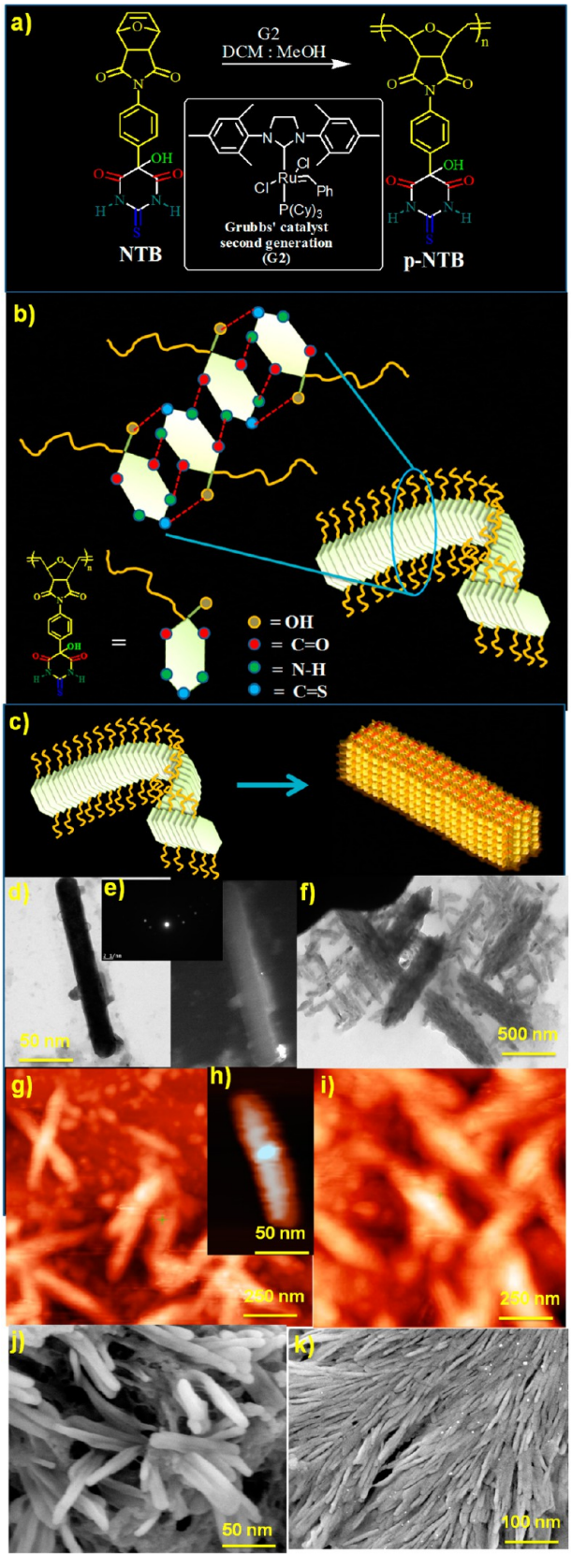

Figure 1. Rod-like aggregates are observed from the solution of 1 wt % **p-NTB** in THF: (a) A schematic representation for **p-NTB**; (b, c) A cartoon representation; (d, f) TEM images; (e) SAED pattern observed for the rods in the TEM; (g–i) AFM images; (j, k) SEM images.

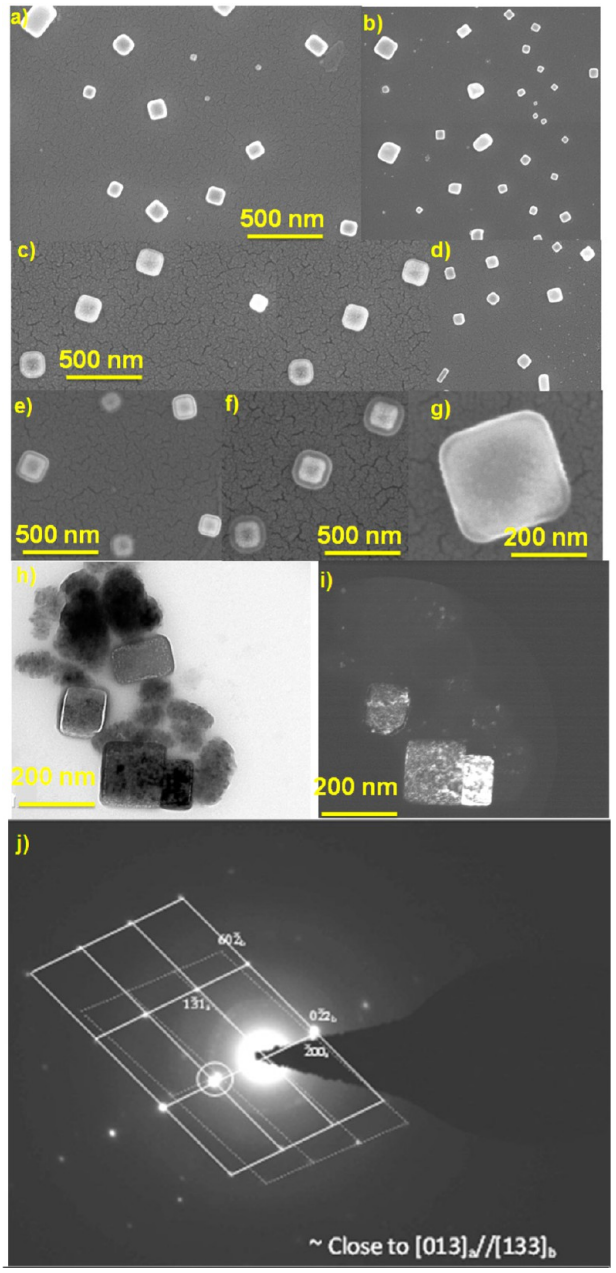

Figure 2. Cube-like aggregates are observed from the solution of 1 wt % **p-NTB** in THF–water (1:1 mixture): (a–g) SEM images; (h, i) TEM images; (j) SAED pattern observed for the cubes in the TEM.

systems (THF–water and THF–MeOH) for this amphiphilic homopolymer were used to investigate. Synthesis and characterization of **p-NTB** were discussed in the Supporting Information (Figure 1a and SI Figures S2 and S3). The molecular weight of the polymer was 38500 (M_n) and its PDI was 1.04. To study the self-assembly, **p-NTB** in tetrahydrofuran (THF) solution was first analyzed by dynamic light scattering (DLS) technique. Light scattering measurements suggested the presence of aggregates in THF with an average diameter of 39 nm (SI, Figure S4), which was in excellent agreement with the various Microscope results (Figure 1). To explore the correlation between the assemblies in the THF and a dry sample on the substrate, the aggregates of the amphiphilic homopolymers were studied by AFM, SEM, and TEM. A histogram of several structures, collected from various AFM

dx.doi.org/10.1021/mz4005524 | ACS Macro Lett. 2014, 3, 44–50

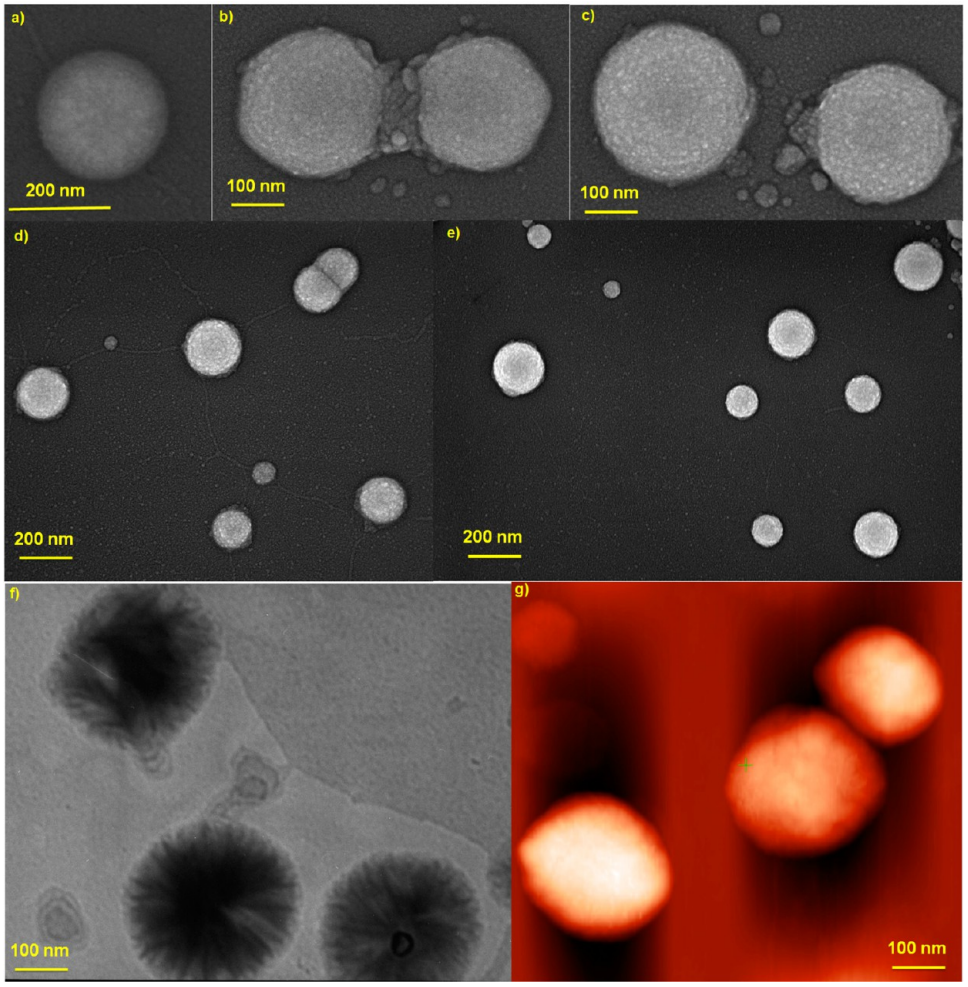

Figure 3. Sphere-like aggregates are observed from the solution of 1 wt % **p-NTB** in THF−MeoH (1:1 mixture): (a−e) SEM images; (f) TEM images; (g) AFM images.

samples, revealed an average diameter of 30 nm with a rod-like shape. SEM images (Figure 1j,k) also revealed that the structures had diameters of around 30 nm with a rod shape. A series of TEM images were collected and a representative image, as shown in Figure 1d (stained with RuO_4), confirmed that the structures previously observed by AFM and SEM were rods. The sizes and diameters of these rods observed by TEM were similar to those visualized by AFM and SEM.

Next, we envisioned that the presence of the chemical heterogeneity in the structure would enable the self-assembly of **p-NTB** in selective solvents. We first studied the self-assembly of **p-NTB** in polar THF−water mixtures to test our prediction. The slow addition of water to **p-NTB** dissolved in THF reduced the solubility of hydrophobic norbornene backbone of **p-NTB**, thus, leading to their spontaneous organization of **p-NTB** into aggregates. The overall concentration of the solution was maintained at 1 wt % of **p-NTB**. The size of the aggregate was measured by DLS instrument. The observed size was 260 nm (SI, Figure S5). The same solution was tested for its morphology characterization. It was very interesting to observe from the SEM analysis that the observed aggregates in the THF−water mixture were unique cube-like structure as shown in Figure 2a−g. When water was slowly added into THF solution of the **p-NTB** to make the overall solvent composition 1:1, formation of large intermediate aggregates was expected. During this process, THF and water were trapped inside the aggregates. But at the initial stage, the THF content was relatively high. Due to this, the viscosity of the core of an aggregate was low, hence, the mobility of the chain was very high. Because of this, the solvent diffusion was expected to be high, which resulted in liquid−liquid phase separation.[11a] As the water content increased to reach the 1:1 level, the viscosity of the core became higher due to polar groups interaction and mobility of the chains became lower due to the extraction of THF from the aggregates. We believed that this could be the possible reason to reach a stable and unique cubic structure observed in the SEM analysis.

The cube-like hierarchical aggregate formation was further confirmed by the TEM (Figure 2h−j) as well as AFM (SI, Figure S7) analysis. The selected area electron diffraction (SAED) observed from the cube-like aggregates is shown in (Figure 2j). From the observed SAED pattern, the hierarchical self-assembly of amphiphilic **p-NTB** polymers was confirmed. Three types of patterns could be identified from the observed diffraction pattern. A ring pattern appearing in the center was due to smaller aggregates, in our case, it could be from the rod-like aggregates (Figures 2j and 1e). The fundamental (primary) reflections, appearing as bright spots in pattern, were from the single cube-like aggregates (corresponding image appear very bright in dark field image, Figure 2i). Finally, the secondary reflections which were appearing as less bright spots in pattern from another single crystals (corresponding image appear less

dx.doi.org/10.1021/mz4005524 | *ACS Macro Lett.* 2014, 3, 44−50

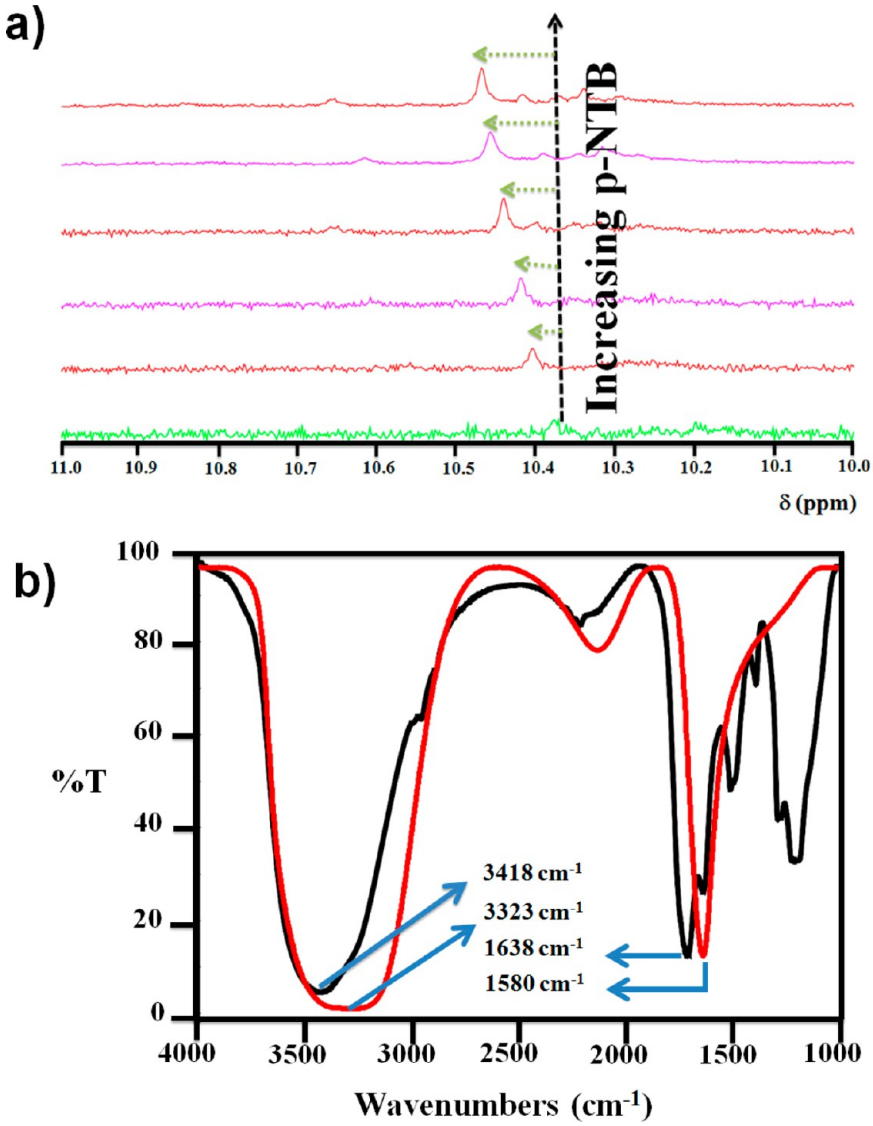

Figure 4. (a) Selected area of ^{1}H NMR spectra of **p-NTB** in DMSO-d^6; (b) FT-IR spectra of **p-NTB** in solid state (black) as well as in water (red).

bright in dark field image, Figure 2i). Based on these observation, we hypothesized that the fundamental reflections were close to $[013]_a$ zone axis and the secondary reflections were close to $[133]_b$ zone axis. Since the observed pattern was a composite diffraction pattern from the cube-like aggregates, which were parallel to each other (Figure 2h), we proposed that the orientation relationship could be close to a cubic structure ($[013]_a//[133]_b$). It was very interesting to observe the uniform cube-like hierarchical organization of **p-NTB** in the THF−water mixture system.

Motivated by the hierarchical organization of **p-NTB** in THF−water system, we wanted to explore the self-assembly of **p-NTB** in relatively less polar solvent mixture system. Toward this motivation, THF−MeOH solvent mixture was explored. First the **p-NTB** was dissolved in THF and then MeOH was added carefully to maintain the 1:1 ratio between THF and MeOH. Again the concentration of **p-NTB** in this study was also maintained to be 1 wt %. Then the solution was first tested for the aggregation behavior using DLS instrument. The size of the aggregates was observed as 254 nm in the DLS instrument (SI, Figure S6). With the addition of methanol to **p-NTB** in THF, **p-NTB** self-assembled into reverse spherical aggregates (Figure 3). The formation of such structures could be explained by minimization of the interfacial energy between the hydrophilic blocks and surrounding medium through lateral packing and aligning of rods. We believed that the hydrophilic blocks were forced to squeeze together, and the hydrophobic blocks were exposed to the surrounding nonpolar environment to stabilize the structures. Due to this sphere aggregates were therefore obtained. The formation of the spheres were first observed in SEM (Figure 3a−e) and confirmed by TEM (Figure 3f) and AFM (Figure 3g). To explore it further, various control experiments by varying the solvent ratios as well as solvent mixtures were done (SI, Figure S8). The method of nonsolvent addition (rapid, slow, effect of mixing) to **p-NTB** polymer in THF was also explored and tabulated (SI, Figure S8). When it was 3:1 (THF−MeOH), the rod-like aggregates were arranged like a sheet where as in (THF−water) a dense population of rod-like aggregates were seen. The rapid addition of hexane (nonsolvent) to **p-NTB** in THF did not produce any interesting structures. Interestingly, 1:3 ratio of THF−MeOH provided a flower-like arrangement of the rods. 1:3 ratio of THF−water provided an intense packing of cube aggregates. From the above control experiments, it was interesting to note

dx.doi.org/10.1021/mz4005524 | *ACS Macro Lett.* 2014, 3, 44−50

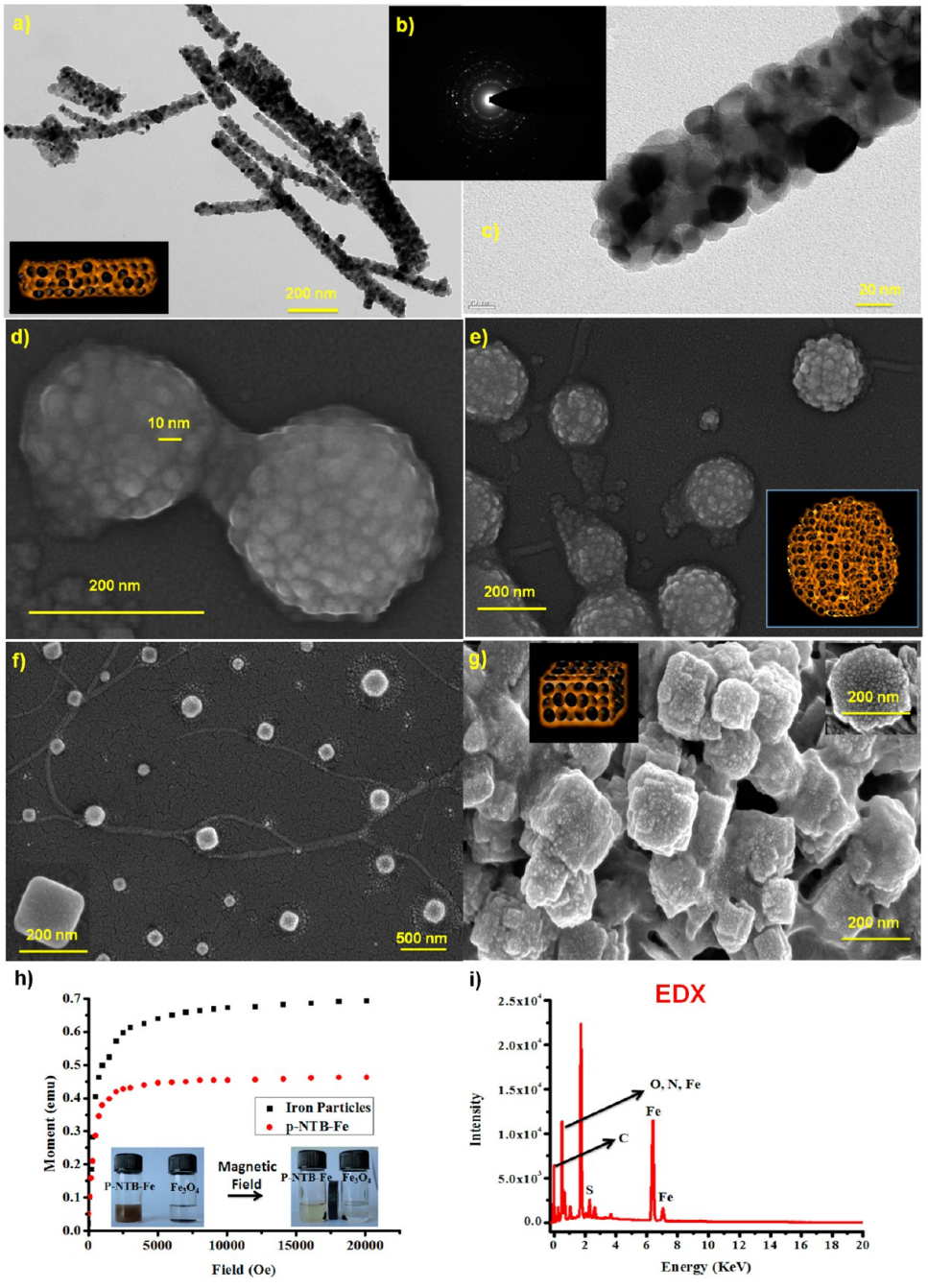

Figure 5. Magnetic particles loaded **p-NTB** aggregates are shown here: (a–c) TEM images; (d–g) SEM images; (h) SQUID data (Inset: demonstration of the movement of the magnetic particle loaded aggregates toward the external magnetic field); (i) A representative EDX data for the magnetic particle loaded aggregates.

that the unique shapes were observed only in the case of 1:1 mixing. In both solvent mixture systems, the hydrophilic units were densely packed to avoid interaction with surrounding nonpolar solvents. Depending on the hydrophilic/hydrophobic balance, **p-NTB** underwent two morphology transitions, varying their structures from rods, to bundle micelles, and eventually to cube-like or sphere-like aggregates. We speculated that the thiobarbiturate motifs in the amphiphilic homopolymer might provide the connections between the different polymer chains, which would also increase the interior viscosity of the aggregates during the formation of cube-like as well as sphere-like aggregates.

Formation of hierarchical superstructures from **p-NTB** prompted us to explore the possibility of hydrogen bonding between thiobarbiturate motifs of **p-NTB**. To prove the involvement of thiobarbiturate motifs in hydrogen bonding, **p-NTB** in water was studied using FT-IR spectroscopy on 1 wt % aqueous solutions (Figure 4b). The presence of strong bands in the spectrum of **p-NTB** at 3323 cm^{-1} (N–H), 1638 cm^{-1} (amide I), and 1580 cm^{-1} (amide II) indicated that barbiturate groups in **p-NTB** were strongly hydrogen bonded.[11b,c] In addition, the shift in the value of stretching frequency between solid state and in solution (water) suggested the presence of strong hydrogen bonding (Figure 4b). The importance of hydrogen bonding in the formation of **p-NTB** nanoaggregates

dx.doi.org/10.1021/mz4005524 | *ACS Macro Lett.* 2014, 3, 44–50

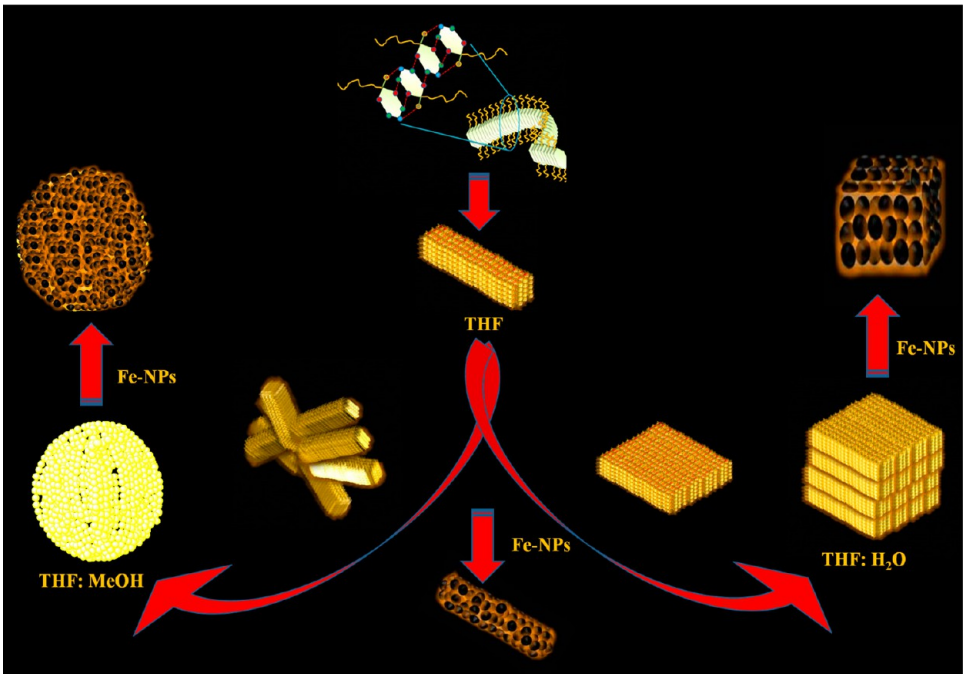

Figure 6. Cartoon representation of overall self-assembly event.

leading to the formation of superstructures was further confirmed by concentration dependent NMR spectroscopy. A linear downfield shifts of amide protons were observed in the ^{1}H NMR spectra of **p-NTB** in dimethyl sulfoxide-d^6 recorded at 25 °C with varying concentrations (2.59×10^{-5} to 25.9×10^{-5} mM), as shown in Figure 4a, (SI, Figure S2). Such downfield shifts of protons with an increase in concentration clearly confirmed the presence of intermolecular hydrogen bonding between thiobarbiturate units (Figure 4a). Further, to study the involvement of thiobarbiturate motifs in hydrogen bonding, a metal binding experiment was carried out. Barbiturates and thiobarbiturates were well-known to bind with copper. To study this effect, copper sulfate solution was added to **p-NTB** solution and its absorbance at 783 nm was monitored (SI, Figure S9). Due to copper binding with **p-NTB**, its absorbance was completely vanished. In another experiment, to a saturated aqueous solution of **p-NTB**, saturated sodium chloride solution was added. An immediate **p-NTB** precipitation was observed and **p-NTB** precipitate was settled down at the bottom of the tube (SI, Figure S10). These two experiments confirmed the hydrogen bonding of thiobarbiturate motifs in **p-NTB**.

In an effort to explore potential applications of these unique structures, their reservoir properties were evaluated by magnetic particles as well as drug-encapsulation studies. For the magnetic particle encapsulation study, 1 wt % of **p-NTB** in THF−water (1:1) solvent mixture was made. A detailed encapsulation procedure has been given in the experimental section in Supporting Information. After the encapsulation, the solutions were tested for the morphological observation. It was very interesting to note that the particle could be loaded in all three forms of the **p-NTB** nanoaggregates, namely, rods, spheres, and cubes. Figure 5a−c show the TEM images of magnetic particle loaded rods. The SAED pattern (Figure 5b) from the magnetite particle encapsulated nanoaggregates indicated that the diffraction pattern was a bcc type atomic ordering.[12a] It was obvious to note that the diffraction pattern from Fe_3O_4 particles was too strong, the diffraction pattern from polymeric nanoaggregates could not be identified separately, as in the case of Figure 2j. Figure 5d,e shows the representative images for the Fe_3O_4 particle loaded spheres, whereas Figure 5f,g shows the Fe_3O_4 particle loaded cubes. Thus, we also studied energy dispersive X-ray spectroscopy (EDX) point scan measurements at different positions along the contour of a magnetic particle loaded **p-NTB** rods (Figure 5i). The observed both K α and L α lines of iron was indicating the presence of iron particles in the same rod-like micelle. Similar results were also obtained for sphere-like as well as cube-like aggregates containing both iron nanoparticles.

The magnetic properties of Fe_3O_4 nanoparticles and **p-NTB-Fe** nanoaggregates were measured by magnetic property measurement system (MPMS) magnetometry at 300 K. A typical magnetization (M) versus applied magnetic field (H) curve at room temperature is shown in Figure 5h. The recorded magnetization for the **p-NTB-Fe** nanoaggregates was 45 emu/g. For Fe_3O_4 particles alone it was recorded as 65 emu/g. The observed 45 emu/g was considered to be excellent magnetization value as it was much higher than the minimum value (10 emu/g) needed for pharmaceutical and biomedical application.[12b,c] We attributed this high magnetic strength from the **p-NTB-Fe** nanoaggregates to the close interaction of the magnetic particles loaded in the **p-NTB-Fe** nanoaggregates. Due to this, magnetostatic pull force could be expected in gradient magnetic field. To test it quickly, the magnetic particle loaded **p-NTB-Fe** nanoaggregates in aqueous solution were introduced to the permanent magnet. It was observed that the magnetic particle loaded nanoaggregates moved toward the permanent magnet in an aqueous solution as shown in the Figure 5h (inset). Similar results were also obtained for sphere-like as well as cube-like aggregates with iron nanoparticles. We believed that this powerful magnetic vector of the nanocarriers would be effectively utilized for magnetic resonance imaging (MRI). The overall self-assembly process of **p-NTB** and magnetic particle loading have been explained in a cartoon representation as shown in Figure 6.

dx.doi.org/10.1021/mz4005524 | *ACS Macro Lett.* 2014, 3, 44−50

Finally, these **p-NTB** aggregates were explored for the usage in drug delivery applications. Toward this goal, encapsulation of doxorubicin (**DOX**) was done with rods, sphere-like as well as cube-like aggregates (see SI experimental section and SI Figure S11). It was interesting to note that maximum drug loading was observed in cubes (68%), followed by spheres (55%) and in rods (34%). The drug release studies in lipophilic environment were demonstrated (SI, Figures S12−15). From the drug release profile, we speculated that the drug was released from the nanoaggregates following a well-known "burst mechanism". We believed that under the acidic conditions, there was a breakage in hydrogen bonding between the barbiturate functionality, which played a very crucial role in forming the aggregates. Most importantly, the original morphologies (such as cube-like or sphere-like) of **p-NTB** aggregates were maintained and no collapsed aggregates were observed during SEM and TEM analysis even after loading the drug and magnetic particles (SI, Figure S16). This suggested the extreme stability of these aggregates after reaching that morphological state. Remarkably, it clearly revealed the extended stability of the observed structures similar to the pioneering work on PRINT technology by DeSimone and co-workers.[13] We envisioned that it could be due to the enhanced stiffness of thiobarbiturate functionality during the packing arrangement.

In summary, we have utilized synthetic amphiphilic homopolymer molecular design with solution conditions that favor self-attraction to produce first rod-like micelles. These rods are further self-assembled to sphere-like, or Cube-shaped, aggregates with a high degree of control and uniformity. We have also demonstrated that this self-assembly of **p-NTB** is solely determined by the properties of the constituent functionality and the nature of solvents. Further we utilized these aggregates for magnetic particle as well as **DOX** encapsulation. **DOX** release from rods, cubes, and spheres like superstructures were demonstrated. To our knowledge, multifunctional cube-like and sphere-like superstructures from the amphiphilic homopolymers and efficient loading of magnetic nanoparticles as well as drug molecules to these superstructures have not been previously reported. This unique and simple approach will allow access to a wide variety of multifunctional nanoaggregates with well-defined morphology.

■ ASSOCIATED CONTENT

Supporting Information

Scheme, synthetic procedure, GPC, DLS, and additional analytical data. This material is available free of charge via the Internet at http://pubs.acs.org.

■ AUTHOR INFORMATION

Corresponding Author

*E-mail: sraja@iiserkol.ac.in.

Notes

The authors declare no competing financial interest.

■ ACKNOWLEDGMENTS

S.R.M. thanks IISER-Kolkata and CSIR, New Delhi, for the research fellowship and R.S. thanks DST, New Delhi, for Ramanujan Fellowship and IISER-Kolkata for the infrastructure. Dr. S. Sankaran and Mr. Joseph Bekman at I.I.T. Madras are acknowledged for the TEM studies. Mr. Ankan Paria and Mr. Kashinath from Carl Zeiss India are also acknowledged for SEM images.

■ REFERENCES

(1) (a) Hartgerink, J. D.; Benish, E.; Stupp, S. I. *Science* **2001**, *294*, 1684. (b) Hill, J. P.; Jin, W.; Kosaka, A.; Fukushima, T.; Ichihara, H.; Shimomura, T.; Ito, K.; Hashizume, T.; Ishii, N.; Aida, T. *Science* **2004**, *304*, 1481. (c) Lee, H.-K.; Park, K. M.; Jeon, Y. J.; Kim, D.; Oh, D. H.; Kim, H. S.; Park, C. K.; Kim, K. *J. Am. Chem. Soc.* **2005**, *127*, 5006. (d) Seo, S. H.; Chang, J. Y.; Tew, G. N. *Angew. Chem., Int. Ed.* **2006**, *45*, 7526.

(2) (a) Discher, D. E.; Eisenberg, A. *Science* **2002**, *297*, 967. (b) Holowka, D. J.; Pochan, J.; Deming, T. J. *J. Am. Chem. Soc.* **2005**, *127*, 12423. (c) Zhao, W.; Chen, D.; Hu, Y.; Grason, G. M.; Russell, T. P. *ACS Nano* **2011**, *5*, 486. (d) Basak, D.; Ghosh, S. *ACS Macro Lett.* **2013**, *2*, 799. (e) Zhang, B.; Zhang, H.; Li, Y.; Hoskins, J. N.; Grayson, S. M. *ACS Macro Lett.* **2013**, *2*, 845. (f) Ghosh, S.; Basu, S.; Thayumanavan, S. *Macromolecules* **2006**, *39*, 5595.

(3) Vriezema, D. M.; Aragones, M. C.; Elemans, J. A. A. W.; Cornelissen, J. J. L. M.; Rowan, A. E.; Nolte, R. J. M. *Chem. Rev.* **2005**, *105*, 1445.

(4) (a) Aida, T.; Meijer, E. W.; Stupp, S. I. *Science* **2012**, *335*, 813. (b) Jain, S.; Bates, F. S. *Science* **2003**, *300*, 460.

(5) (a) Ma, Y.; Kolotuchin, S. V.; Zimmerman, S. C. *J. Am. Chem. Soc.* **2002**, *124*, 13757. (b) Jiao, D.; Geng, J.; Loh, X. J.; Das, D.; Lee, T.-C.; Scherman, O. A. *Angew. Chem., Int. Ed.* **2012**, *51*, 9633.

(6) (a) Lee, M.; Lee, S.-J.; Jiang, L.-H. *J. Am. Chem. Soc.* **2004**, *126*, 12724. (b) Bellomo, E. G.; Wyrsta, M. D.; Pakstis, L.; Pochan, D. J.; Deming, T. J. *Nat. Mater.* **2004**, *3*, 244. (c) Du, J.; Tang, Y.; Lewis, A. L.; Armes, S. P. *J. Am. Chem. Soc.* **2005**, *127*, 17982. (d) Mahalik, J. P.; Muthukumar, M. *J. Chem. Phys.* **2012**, *136*, 135101. (e) Muthukumar, M.; Ober, C. K.; Thomas, E. L. *Science* **1997**, *277*, 1225.

(7) (a) Geng, Y.; Dalhaimer, P.; Cai, S. S.; Tsai, R.; Tewari, M.; Minko, T.; Discher, D. E. *Nat. Nanotechnol.* **2007**, *2*, 249. (b) Nishiyama, N. *Nat. Nanotechnol.* **2007**, *2*, 203.

(8) (a) Wang, H.; Wang, X. S.; Winnik, M. A.; Manners, I. *J. Am. Chem. Soc.* **2008**, *130*, 12921. (b) Walther, A.; Yuan, J.; Abetz, V.; Muller, A. H. E. *Nano Lett.* **2009**, *9*, 2026. (c) Wang, M. F.; Zhang, M.; Li, J.; Kumar, S.; Walker, G. C.; Scholes, G. D.; Winnik, M. A. *ACS Appl. Mater. Interfaces* **2010**, *2*, 3160. (d) Mai, Y. Y.; Eisenberg, A. *Macromolecules* **2011**, *44*, 3179. (e) Zhu, J. T.; Hayward, R. C. *J. Am. Chem. Soc.* **2008**, *130*, 7496.

(9) Chebotareva, N.; Paul, H. H. B.; Frederik, P. M.; Sommerdijka, N. A. J. M.; Sijbesma, R. P. *Chem. Commun.* **2005**, *39*, 4967.

(10) (a) Mane, S. R.; Rao, V. N.; Shunmugam, R. *ACS Macro Lett.* **2012**, *1*, 482. (b) Mane, S. R.; Rao, V. N.; Chatterjee, K.; Dinda, H.; Nag, S.; Kishore, A.; Das Sarma, J.; Shunmugam, R. *Macromolecules* **2012**, *45*, 8037.

(11) (a) Liu, X. Y.; Kim, J. S.; Wu, J.; Eisenberg, A. *Macromolecules* **2005**, *38*, 6749. (b) Yilgor, E.; Burgaz, E.; Yurtsever, E.; Yilgor, I. *Polymer* **2000**, *41*, 849. (c) Coleman, M. M.; Sobkowiak, M.; Pehlert, G. J.; Painter, P. C.; Iqbal, T. *Macromol. Chem. Phys.* **1997**, *198*, 117.

(12) (a) Monson, T. C.; Venturini, E. L.; Petkov, V.; Ren, Y.; Lavin, J. M.; Huber, D. L. *J. Magn. Magn. Mater.* **2013**, *331*, 156. (b) Kong, S. D.; Zhang, W.; Lee, J. H.; Brammer, K.; Lal, R.; Karin, M.; Jin, S. *Nano Lett.* **2010**, *10*, 5088. (c) He, X.; Wu, X.; Cai, X.; Lin, S.; Xie, M.; Zhu, X.; Yan, D. *Langmuir* **2012**, *28*, 11929.

(13) Chu, K. S.; Hasan, W.; Rawal, S.; Walsh, M. D.; Enlow, E. M.; Luft, J. C.; Bridges, A. S.; Kuijer, J. L.; Napier, M. E.; Zamboni, W. C.; Desimone, J. M. *Nanomedicine* **2013**, *9*, 686.